MJFAS
Malaysian Journal of Fundamental and Applied Sciences

Fathi *et al.* | Malaysian Journal of Fundamental and Applied Sciences, Vol. 20 (2024) 1398-1409

RESEARCH ARTICLE

Valency-Based Molecular Descriptor on Structural Property Relationship of Ni Tetrathiafulvalene Tetrathionate

Abdelli Fathi[a], Sahaya Vijay J[b], Mohamad Nazri Husin[a*], Tony Augustine[c]

[a]Special Interest Group on Modeling and Data Analytics (SIGMDA), Faculty of Computer Science and Computer, Universiti Malaysia Terengganu, Kuala Nerus 21030, Terengganu, Malaysia; [b]Department of Mathematics, Vellore Institute of Technology, Vellore 632014, India; [c]Viswajyothi College of Engineering and Technology, Vazhakulam-686670 Kerala, India

Abstract Induced by quantitative structural relationships, valency-based topological indices have been investigated for predicting the structural properties of Ni Tetrathiafulvalene tetrathionate (NiTTFtt) like 2D sheet. Through the use of topological indices, the Kubelka-Munk function for bad gap energy, vibrational frequencies of IR spectroscopy, and graph energy of NiTTFtt like 2D sheet are calculated. The structural features studied have applications such as biosensing, drug discovery, chemical graph theory, machine learning, and more. This main study focused on deriving expressions and numerical values of valency-based topological indices for NiTTFtt like 2D sheet. Additionally, we employed technique to calculate the Kubelka-Munk function values linearly increase when obtained directly from numerical values of valency-based topological indices. Finally, for investigating the properties of NiTTFtt like 2D sheet, statistical correlation analysis shows a significant correlation with vibrational frequencies.

Keywords: Ni Tetrathiafulvalene tetrathionate, edge partition, valency-based molecular descriptors, structural-properties, topological indices.

Introduction

Technologies ranging from displays to flexible electronics are supported by conducting organic materials, such as doped organic polymers, developing coordination polymers, and molecular conductors. Chemical doping is used to adjust the electronic structure of organic materials that are typically insulators to achieve high electrical conductivity. Moreover, crystallinity is necessary for metallic behavior even in materials that are innately conductive, such as single-component molecular conductors [1-3]. Commercial conducting polymers, on the other hand, are frequently made intentionally amorphous to help with processability and durability. There are no intrinsically conducting organic materials that retain high conductivity when disordered, even though using molecular design to create high conductivity in undoped amorphous materials would permit flexible and resilient conductivity in many applications. Though they need to be carefully fabricated, inorganic glassy metals have been found. Moreover, it is yet unknown how geometric disorder and metallic behavior interact in these materials. Metallic behavior is traditionally associated with periodicity, which gives birth to a well-defined band structure [4-6].

A completely amorphous coordination polymer, Ni Tetrathiafulvalene tetrathionate (NiTTFtt), exhibits intrinsic electrical conductivity, maintaining high conductivity even in disordered state and displaying deep intrinsic metallic conductivity. NiTTFtt demonstrates significantly high electronic conductivity (1280 S/cm). Cutting-edge theory analysis reveals that its molecular properties are enabled by strong molecular correlation. This material, tailored for near-infrared wavelengths, serves as a photo thermoelectric for solar energy harvesting applications. Reduced materials derived from the glassy-metallic conductivity of NiTTFtt exhibit physical characteristics more akin to p-type semiconductors. Despite NiTTFtt's amorphous nature, John Anderson and colleagues constructed a structural model based on experimental data. NiTTFtt compounds show promise in sensing technologies,

***For correspondence:**
nazri.husin@umt.edu.my

Received: 31 Aug. 2024
Accepted: 21 Oct. 2024

electronics, materials research, energy storage, and other fields. These qualities are actively being investigated for real-world applications across various sectors. This study demonstrates physical properties consistent with p-type semiconductors for (m,n)-types glassy metallic conductivity NiTTFtt (See Figure 1b) [7]. Because of its structural amorphousness, NiTTFtt cannot have a classical band structure. However, through characterization of NiTTFtt indicates a metallic nature and strong conductivity. The substantial overlap between the molecular units of NiTTFtt, which is insensitive to structural deformation, allows for the presence of this metallic behavior. There is still uncertainty regarding the precise mechanism of charge transport at the limit of no structural ordering, as evidence suggests both band-like and hopping transport [3, 7-9]. NiTTFtt demonstrates that organic materials made of much more complicated and adjustable molecular building blocks exhibit the same intriguing characteristics. Regardless, NiTTFtt offers exceptional thermally and aerobically stable conductivity due to the contrast between its metallic nature and disorder. These findings indicate that metallic character can be achieved even in fully amorphous materials by using molecular units with significant overlap and strong electronic delocalization. With structural information on NiTTFtt in hand, we proceeded to investigate its electronic properties.

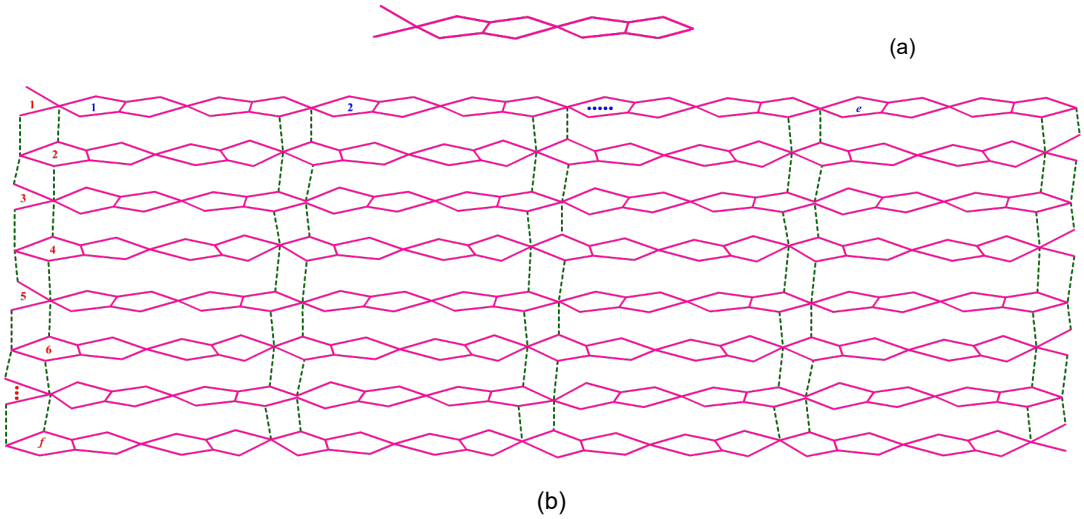

Figure 1. Ni Tetrathiafulvalene tetrathionate (NiTTFtt), a) Unit cell, b) NiTTFtt like 2D sheet with *m*, *n* parameters

In this article we consider the unit cell of NiTTFtt like 2D sheet (See Figure 1a) and converted to molecular graph. Generally, molecular graphs contain atoms and bonds which should be considered as vertices and bonds. In this study, atoms and bonds of NiTTFtt like 2D sheet are considered as vertices and edges. Also, we consider the growth of the structure with parameters m and n (See Figure 1b). Using the graph techniques we find generalized pattern for valency based 1topological indices of NiTTFtt like 2D sheet and its numerical values. Also, calculate the Kubelka-Munk function, vibrational frequency and graph energy.

A subfield of discrete mathematics known as “chemical graph theory” makes it easier to compute topological descriptors of molecular structures. These descriptors can subsequently be utilized to forecast the physical and chemical characteristics of complicated systems like NiTTFtt like 2D sheet. In molecular graphs, the edges represent chemical bonds, and the vertices represent the atoms that make up the molecular structure. Since the structures of molecules determine their properties, real numbers obtained from the corresponding molecular graphs are known as graph invariants or, more commonly, structural descriptors (topological indices) [10-13]. To create prediction models that cut down on costly and time-consuming laboratory trials, a variety of topological indices have developed over time based on the path distance and degree of the vertices [14].

Materials and Methods

A simple graph G has a set of vertices V which are linked by a set of edges E. The cardinality of V is r and the cardinality of E is s. A vertex $u \in V(G)$ to a vertex $v \in V(G)$ is called the distance between u and v denoted by $d(u,v)$. The cardinality of collection of vertices x is called the degree of a vertex u of G if $d(u,x) = 1$, where $u, x \in V(G)$ [15, 16]. A partition of a graph G if it contains a collection of disjoint edges of G. A topological index is a numerical value that describes the topology of a graph and is unaffected by graph automorphism. The following topological descriptors from Table 1 are used in this study to achieve our proposed results [17, 18].

Table 1. Topological Descriptor (TD) Formula [19-33]

S. No.	TD	Formula
1	First Zagreb index	$M_1(G) = \sum_{v \in V(G)} (d_u + d_v)$
2	Second Zagreb index	$M_2(G) = \sum_{uv \in E(G)} d_u d_v$
3	Reduced second Zagreb index	$RM_2(G) = \sum_{uv \in E(G)} (d_u - 1)(d_v - 1)$
4	Hyper Zagreb index	$HM(G) = \sum_{uv \in E(G)} (d_u + d_v)^2$
5	Augmented Zagreb index	$AZ(G) = \sum_{uv \in E(G)} \left[\frac{d_u d_v}{d_u + d_v - 2}\right]^3$
6	Randic index	$R(G) = \sum_{uv \in E(G)} \left[\frac{1}{\sqrt{d_u d_v}}\right]$
7	Reciprocal Randic index	$RR(G) = \sum_{uv \in E(G)} \sqrt{d_u d_v}$
8	Reduced Reciprocal Randic index	$RRR(G) = \sum_{uv \in E(G)} \sqrt{(d_u - 1)(d_v - 1)}$
9	Harmonic index	$H(G) = \sum_{v \in V(G)} \frac{2}{d_u + d_v}$
10	Sum-Connectivity index	$SC(G) = \sum_{uv \in E(G)} \frac{1}{\sqrt{d_u + d_v}}$
11	Atom Bond Connectivity index	$ABC(G) = \sum_{uv \in E(G)} \sqrt{\frac{d_u + d_v - 2}{d_u d_v}}$
12	Forgotten index	$F(G) = \sum_{uv \in E(G)} d_u^2 + d_v^2$
13	Geometric Arithmetic index	$GA(G) = \sum_{uv \in E(G)} \frac{2\sqrt{d_u d_v}}{d_u + d_v}$
14	Bi-Zagreb Index	$BM(G) = \sum_{uv \in E(G)} (d_u + d_v + d_u d_v)$
15	Tri-Zagreb index	$TM(G) = \sum_{uv \in E(G)} \frac{\sqrt{d_u d_v}(d_u d_v)}{2}$
16	Geometric Harmonic index	$GH(G) = \sum_{uv \in E(G)} (d_u^2 + d_v^2 + d_u d_v)$
17	Geometric Bi-Zagreb index	$GBM(G) = \sum_{uv \in E(G)} \frac{\sqrt{d_u d_v}}{d_u + d_v + d_u d_v}$
18	Geometric Tri-Zagreb index	$GTM(G) = \sum_{uv \in E(G)} \frac{\sqrt{d_u d_v}}{d_u^2 + d_v^2 + d_u d_v}$

S. No.	TD	Formula
19	Harmonic-Geometric index	$HG(G) = \sum_{uv\in E(G)} \frac{2}{\sqrt{d_u d_v}(d_u d_v)}$
20	Harmonic Bi-Zagreb index	$HBM(G) = \sum_{uv\in E(G)} \frac{2}{(d_u d_v)(d_u + d_v + d_u d_v)}$
21	Harmonic Tri-Zagreb index	$HTM(G) = \sum_{uv\in E(G)} \frac{2}{(d_u d_v)(d_u^2 + d_v^2 + d_u d_v)}$
22	Bi-Zagreb Geometric index	$BMG(G) = \sum_{uv\in E(G)} \frac{(d_u + d_v + d_u d_v)}{\sqrt{d_u d_v}}$
23	Bi-Zagreb Harmonic index	$BMH(G) = \sum_{uv\in E(G)} \frac{(d_u d_v)(d_u + d_v + d_u d_v)}{2}$
24	Tri-Zagreb Geometric index	$TMG(G) = \sum_{uv\in E(G)} \frac{(d_u^2 + d_v^2 + d_u d_v)}{\sqrt{d_u d_v}}$
25	Tri-Zagreb Harmonic index	$TMH(G) = \sum_{uv\in E(G)} \frac{(d_u d_v)(d_u^2 + d_v^2 + d_u d_v)}{2}$

Results

In this section, first, twenty-five degree-based topological indices are enumerated for NiTTFtt 2D sheet. The unit cell of NiTTFtt like 2D sheet are formed in row and column wise like 2D sheet (See Figure 1 and its notation is denoted by NiTTFtt (m, n)), where n represents a linear formation of NiTTFtt 2D sheet (NiTTFtt 2D (*1*, *n*) and m represents a construction of sequence of NiTTFtt 2D (*1*, *n*). Throughout this paper, we used this NiTTFtt (m, n) notation instead of Ni Tetrathiafulvalene Tetrathiolate like 2D sheet. Throughout this article, we use m and n which are represents row and column of NiTTFtt 2D like 2D sheet. Atoms and bonds of NiTTFtt 2D like 2D sheets are called vertices and edges with respect to molecular graph definition. The total number of vertices and edges of NiTTFtt (m, n) are $14mn + 3m$ and $20mn + 4m - 2n - 2$. A potential graph theory method such as edge set partition is used to enumerate degree-based topological indices expressions. First edge set E is divided into different subsets or classes with respect to end vertices of each edge to calculate degree based topological descriptors of NiTTFtt (m, n) using MATLAB (See Table 3). And the edge set partitions of NiTTFtt are given in below Table 2. Numerous representations of a graph is always denoted as G. In the same way, throughout this article, NiTTFtt (m, n) is represent as G. The results of 25 degree based topological indices are used to predict significant rates law such as Kubelka-Munk [34], Vibrational frequency [35] for IR spectroscopy and graph energy [36] for graph properties in upcoming sections.

Table 2. Edge set partitions of NiTTFtt (m, n)

Set of edge partitions (E_γ)	$\lvert E_\gamma \rvert$
$(1, 5)$	2
$(2, 3)$	$6mn + 2n + 4$
$(2, 4)$	$4mn + 2m - 4$
$(2, 5)$	$6n$
$(2, 6)$	$2mn - 4n + 2m - 4$
$(3, 3)$	$4mn + 2m + 4$
$(3, 4)$	$2m - 4$
$(3, 5)$	$4n - 2$
$(3, 6)$	$4mn - 8n - 2m + 4$

Theorem 1. Let G be Ni Tetrathiafulvalene tetrathionate 2D sheet NiTTFtt (m, n). Then

1. $M_1(G) = 24m - 8n + 130mn - 20.$
2. $M_2(G) = 28m - 42n + 200mn - 34.$
3. $RM_2(G) = 8m - 32n + 90mn - 34.$
4. $HM(G) = 136m - 232n + 890mn - 156.$

5. $AZ(G) = \frac{1099408m}{42875} - \frac{205713n}{10976} + \frac{1150143mn}{5488} - \frac{16358931}{686000}$.
6. $R(G) = \frac{2n}{3} + \frac{\sqrt{2}(2m+4mn-4)}{4} + \frac{\sqrt{6}(2n+6mn+4)}{6} + \frac{3\sqrt{10n}}{5} + \frac{4mn}{3} + \frac{2\sqrt{5}}{5} + \frac{\sqrt{3}(2m-4)}{6} + \frac{5\sqrt{15}(4n-2)}{15} + \frac{\sqrt{3}(2m-4n+2mn-4)}{6} - \frac{\sqrt{2}(2m+8n-4mn-4)}{6} + \frac{2}{3}$.
7. $RR(G) = 6n + 2\sqrt{2}(2m + 4mn - 4) + \sqrt{6}(2n + 6mn + 4) + 6\sqrt{10}n + 12mn + 2\sqrt{5} + 2\sqrt{3}(2m - 4) + 15\sqrt{15}(4n - 2) + 2\sqrt{3}(2m - 4n + 2mn - 4) - 3\sqrt{2}(2m + 8n - 4mn - 4) + 6$.
8. $RRR(G) = 16n + \sqrt{3}(2m + 4mn - 4) + \sqrt{2}(2n + 6mn + 4) + 8mn + \sqrt{6}(2m - 4) + 2\sqrt{2}(4n - 2) + \sqrt{5}(2m - 4n + 2mn - 4) - \sqrt{10}(2m + 8n - 4mn - 4) + 4$.
9. $H(G) = \frac{163m}{126} + \frac{442n}{315} + \frac{581mn}{90} - \frac{97}{630}$.
10. $SC(G) = \frac{\sqrt{2}\sqrt{3}}{3} - \frac{8n}{3} - \frac{2m}{3} + \frac{\sqrt{6}(2m+4mn-4)}{6} + \frac{\sqrt{6}(2n+4mn+2)}{6} + \frac{\sqrt{5}(2n+6mn+4)}{5} + \frac{6\sqrt{7}n}{7} + \frac{4mn}{3} + \frac{\sqrt{7}(2m-4)}{7} + \frac{\sqrt{2}(4n-2)}{4} + \frac{\sqrt{2}(2m-4n+2mn-4)}{4} + \frac{4}{3}$.
11. $ABC(G) = \frac{4n}{3} + \frac{\sqrt{2}(2m+4mn-4)}{2} + \frac{\sqrt{2}(2n+6mn+4)}{2} + 3\sqrt{2}n + \frac{8mn}{3} + \frac{4\sqrt{5}}{5} + \frac{\sqrt{2}(2m-4n+2mn-4)}{2} + \frac{\sqrt{3}\sqrt{5}(2m-4)}{6} + \frac{\sqrt{2}\sqrt{5}(4n-2)}{5} - \frac{3\sqrt{2}\sqrt{7}(2m+8n-4mn-4)}{7} + \frac{4}{3}$.
12. $F(G) = 80m - 148n + 490mn - 88$.
13. $IS(G) = \frac{107m}{21} - \frac{37n}{70} + \frac{443mn}{15} - \frac{1879}{420}$.
14. $BM(G) = 52m - 50n + 330mn - 54$.
15. $TM(G) = 108M - 190N + 690MN - 122$.
16. $GH(G) = 27n + 8\sqrt{2}(2m - 4n + 2mn - 4) + 3\sqrt{6}(2n + 6mn + 4) + 30\sqrt{10}n + 54mn + 5\sqrt{5} + 12\sqrt{3}(2m - 4) + \frac{15\sqrt{15}(4n-2)}{2} + 12\sqrt{3}(2m - 4n + 2mn - 4) - 27\sqrt{2}(2m + 8n - 4mn - 4) + 27$.
17. $GBM(G) = \frac{2n}{5} + \frac{\sqrt{2}(2m+4mn-4)}{7} + \frac{\sqrt{6}(2n+6mn+4)}{11} + \frac{6\sqrt{10}n}{17} + \frac{4mn}{5} + \frac{2\sqrt{5}}{11} + \frac{2\sqrt{3}(2m-4)}{19} + \frac{15\sqrt{15}(4n-2)}{27} + \frac{\sqrt{2}\sqrt{3}(2n+6mn+4)}{15} + \frac{6\sqrt{2}\sqrt{5}n}{35} + \frac{2}{9}$.
18. $GTM(G) = \frac{2n}{9} + \frac{\sqrt{2}(2m+4mn-4)}{14} + \frac{\sqrt{6}(2n+6mn+4)}{19} + \frac{2\sqrt{10}n}{13} + \frac{4mn}{9}$.
19. $HG(G) = \frac{2n}{9} + \frac{2\sqrt{2}(2m+4mn-4)}{12} + \frac{4mn}{9} + \frac{2\sqrt{5}}{15} + \frac{\sqrt{3}(2m-4)}{21} + \frac{\sqrt{15}(4n-2)}{60} + \frac{\sqrt{3}(2m-4n+2mn-4)}{24} - \frac{\sqrt{2}(2m+8n-4mn-4)}{27} + \frac{\sqrt{2}\sqrt{3}(2n+6mn+4)}{15} + \frac{6\sqrt{2\sqrt{5}n}}{35} + \frac{2}{9}$.
20. $HBM(G) = \frac{19939m}{323190} + \frac{1230731n}{10451430} + \frac{129343mn}{840294} + \frac{3621713}{40883535}$.
21. $HTM(G) = \frac{64907m}{2181816} + \frac{1949089n}{29410290} + \frac{157441mn}{840294} + \frac{3204859289}{67467205260}$.
22. $BMG(G) = 10n + \frac{7\sqrt{2}(2m+4mn-4)}{2} + \frac{11\sqrt{6}(2n+6mn+4)}{6} + \frac{51\sqrt{10}n}{5} + 20mn + \frac{22\sqrt{5}}{5} + \frac{19\sqrt{3}(2m-4)}{6} + \frac{23\sqrt{15}(4n-2)}{15} + \frac{10\sqrt{3}(2m-4n+2mn-4)}{3} - \frac{9\sqrt{2}(2m+8n-4mn-4)}{2} + 10$.
23. $HBM(G) = 94M - 1023N + 1904MN - 211$.
24. $TMG(G) = 18n + 7\sqrt{2}(2m + 4mn - 4) + \frac{19\sqrt{6}(2n+6mn+4)}{6} + \frac{117\sqrt{10}n}{5} + 36mn + \frac{62\sqrt{5}}{5} + \frac{37\sqrt{3}(2m-4)}{6} + \frac{49\sqrt{15}(4n-2)}{15} + \frac{26\sqrt{3}(2m-4n+2mn-4)}{3} - \frac{21\sqrt{2}(2m+8n-4mn-4)}{2} + 18$.
25. $HTM(G) = 158m - 2787n + 4168mn - 425$.

Applications to Topological Descriptor of Nittftt Like 2D Sheet with m, n Parameters

Ni Tetrathiafulvalene Tetrathiolate like 2D sheet (NiTTFtt (m,n)) is characterized with yielding topological descriptors expressions in the above sections which would be make QSPR to predict the properties of NiTTFtt (m,n). Adjacency matrices of these structure also contain a wealth of topological data that can be used in machine learning to analyze the spectroscopies and stabilities of these NiTTFtt (m,n). In the upcoming sections, the graph energy, Kubelka-Munk function and vibrational frequency, including are calculated from the combinatorial counts of NiTTFtt like 2D sheet and can be used to estimate the kinetic energy, IR spectroscopic and their stabilities for the NiTTFtt like 2D sheet. Using MATLAB, numerical values of degree based topological descriptors are obtained from its expressions (See Theorem 1).

A numeric function derived from topological descriptors of NiTTFtt (m,n) facilities QSPR and QSAR, which are given in the below Tables 3-4.

Table 3. Numerical values of degree-based topological descriptors of NiTTFtt (m, n)

TD	M_1	M_2	RM_2	HM	AZ	R	RR	RRR	H	SC
1	126	152	50	638	192.6274	9.3775	60.9726	33.9237	8.9984	10.4036
2	532	738	296	3212	828.25	32.2925	255.2959	157.9382	311.0619	37.2977
3	1198	1724	722	7566	1883	68.6419	573.438	363.0222	66.0365	80.1711
4	2124	3110	1328	13700	3356.9	118.4257	1015.4	649.1756	113.9222	139.024
5	3310	4896	2114	21614	5250	181.6438	1581.2	1016.4	174.719	213.8563
6	4756	7082	3080	31308	7562.2	258.2964	2270.8	1464.7	248.427	304.668
7	6462	9668	4226	42782	10294	348.3834	3084.2	1994.1	335.046	411.4591
8	8428	12654	5552	56036	13444	451.9047	4021.4	2604.5	434.5762	534.2296
9	10654	16040	7058	71070	17014	568.8604	5082.5	3296	547.0175	672.9795
10	13140	19826	8744	87884	$2.1003e + 04$	699.2506	$6.2674e + 03$	$4.0686e + 03$	672.3698	827.7089
TD	ABC	F	IS	BM	TM	GH	GBM	GTM	HG	HBM
1	15.2027	334	29.6262	278	486	181.8773	5.1639	2.8384	3.4951	764
2	62.6767	1736	122.7929	1270	2474	1088.4	18.4074	9.7777	11.3253	5547
3	145.2831	4118	275.0262	2922	5842	2670.2	39.4891	20.7662	23.6544	14138
4	263.0219	7480	486.3262	5234	10590	4927.3	68.4092	35.804	40.4826	26537
5	415.8932	11822	756.6929	8206	16718	7859.7	105.1676	54.8911	61.8097	42722
6	603.897	17144	1086.1	11838	24226	11467	149.7643	78.0274	87.6358	62759
7	827.0331	23446	1474.6	16130	33114	15750	202.1993	105.213	117.9609	86582
8	1085.3	30728	1922.2	21082	43382	20709	262.4726	136.4479	152.785	114213
9	1378.7	38990	2428.8	26694	55030	26342	330.5842	171.7321	192.1081	145652
10	$1.7072e + 03$	48232	$2.9945e + 03$	32966	68058	32651	406.5342	211.0655	235.9302	180899

Table 4. Numerical values of degree-based topological descriptors of NiTTFtt (m, n)

δ	HTM	BMG	HBM	TMG	TMH
1	1114	110.96780	764	200.8028	1114
2	10989	442.88	5547	856.2392	10989
3	29200	982.2846	14138	1934.8	29200
4	55747	1729.2	26537	3436.5	55747
5	90630	2683.6	42744	5361.2	90630
6	133849	3845.5	62759	7709.1	133849
7	185404	5214.8	86582	10480	185404
8	245295	6791.7	114213	13674	245295
9	313522	8576.1	145652	17292	313522
10	390085	10568	180899	21332	390085

Kubelka Munk Function (KM) of Nittftt (m,n) From Numerical Values of Degree-Based Topological Descriptors

The absorption spectrum is calculated by the Kubelka-Munk (KM) function from reflection spectra [37]. It is also used in the specification and control of appearance in paints and surface coatings [38]. The Kubelka-Munk function is also called the remission function. Maintly, it is obtained from Diffuse Reflectance Spectroscopy (DRS), and this study focuses on optical property prediction [39]. Deriving the KM function from DRS for NiTTFtt like 2D sheet is experimentally difficult because of its complex structures. Therefore, we have derived the Kubelka-Munk function from degree-based topological descriptors values by applying the formula $KM = \frac{1-R^2}{R}$, which can be used in the appearance of paints films. One can use this KM function for NiTTFtt (m,n) to obtain the band gap energy. The obtained KM function values are given in the below Tables 5-6. Observe that each parameter of KM function of NiTTFtt (m,n) is linearly increasing from the scatter plot (See Figures 2-3). From the conclusion of scatter plot, the observation to the readers is that KM function scales are strongly connected with degree based topological indices.

Table 5. Kubelka Munk Function ((KM) of NiTTFtt (m,n) from numerical values

M_1~	KM	M_2~	KM	RM_2~	KM	HM~	KM	AZ~	KM	R~	KM	RR~	KM	RRR~	KM
126	0.03	152	0.09	50	0.25	638	2.27	192.63	0.22	9.38	4.38	60.97	0.12	33.92	0.64
532	1.75	738	2.76	296	0.65	3213	15.08	828.25	3.20	32.29	0.71	255.3	0.47	157.94	0.11
1198	5.03	1724	7.56	722	2.68	7566	36.84	1883	8.44	68.64	0.07	573.44	1.95	363.02	0.95
2124	9.64	3110	14.57	1328	5.68	13700	36.84	3356.9	15.8	118.43	0.01	1015.4	4.13	649.18	2.32
3310	15.57	4896	23.49	2114	9.59	21614	107.07	5250	25.26	181.64	0.18	1581.2	6.94	1016.4	4.13
4756	22.79	7082	34.42	3080	14.42	31308	155.54	7562.2	36.82	258.3	0.49	2270.8	10.38	1464.7	6.36
6462	31.32	9886	47.35	4226	20.14	42782	212.91	10295	50.47	348.38	0.89	3084.2	14.44	1994.1	9.00
8428	41.15	12654	62.27	5552	26.77	56036	279.18	1344 4	66.22	451.9	1.37	4021.4	19.12	2604.5	12.04
10654	52.27	16040	79.20	7058	34.30	71070	354.35	17014	84.07	568.86	1.93	5082.5	24.42	3296	15.5
13140	64.70	19826	98.13	8744	42.73	87884	438.42	21003	104.02	699.25	2.57	6267.2	30.34	4068.6	19.36
H~	KM	SC~	KM	ABC~.	KM	F~	KM	IS~	KM	BM~	KM	TM~	KM	GH~	KM
9.00	4.60	10.4	3.86	15.2	2.36	334	0.82	29.63	0.84	278	0.57	486	1.53	181.88	0.18
31.06	0.76	37.3	0.53	62.68	0.11	1736	7.71	122.79	0.02	1270	5.39	2474	11.39	1088.4	4.49
66.04	0.09	80.17	0.02	145.28	0.07	4118	19.6	275.03	0.56	2922	13.63	5842	28.22	2670.2	12.37
113.92	0.01	139.02	0.05	263.02	0.51	7480	36.41	486.33	1.53	5234	25.18	10590	51.95	4927.3	23.65
174.72	0.16	213.86	0.3	415.89	1.2	11822	58.11	756.69	2.85	8206	40.04	16718	82.59	7859.7	38.3
248.43	0.44	304.67	0.69	603.9	2.1	17144	84.72	1086.1	4.48	11838	58.19	24226	120.13	11467	56.34
335.05	0.82	411.46	1.18	827.03	3.2	23446	116.23	1474.6	6.41	16130	79.65	33114	164.57	15750	77.75
434.58	1.29	534.23	1.76	1085.3	4.47	30728	152.64	1922.2	8.64	21082	104.41	43382	215.91	20709	102.55
547.02	1.83	672.98	2.44	1378.7	5.93	3899 0	193.95	2428.8	11.16	26694	132.47	55030	274.15	26342	130.71
672.37	2.44	827.71	3.2	1707.2	7.57	48232	240.16	2994.5	13.99	32966	163.83	68058	339.29	32651	162.26

Table 6. Kubelka Munk Function ((KM) of NiTTFtt (m, n) from numerical values

GBM~	KM	GTM~	KM	HG~	KM	HBM~	KM	HTM~	KM	BMG~	KM	TMG~	KM	TMH~	KM
5.16	8.71	284	16.63	3.5	13.32	764	2.89	1114	4.61	110.97	0.01	200.8	0.25	1114	4.61
18.41	1.81	9.78	4.16	11.33	3.47	5547	26.74	10989	53.95	442.88	1.33	856.24	3.34	10989	53.95
39.49	0.46	20.77	1.51	23.65	1.23	14138	69.69	29200	145	982.28	3.96	1934.8	8.7	29200	145
68.41	0.07	35.8	0.58	40.48	0.44	26537	131.69	55747	277.74	1729.2	7.67	3436.5	16.2	55747	277.74
105.17	0.00	54.89	0.19	61.81	0.12	427442	212.72	90630	452.15	2683.6	12.44	5361.2	25.82	90630	452.15
149.76	0.08	78.03	0.03	87.64	0.01	62759	312.8	133849	668.25	3845.5	18.24	7709.1	37.55	133849	668.25
202.2	0.26	105.21	0.00	117.96	0.01	86582	431.91	185404	926.02	5214.8	25.08	10480	51.4	185404	926.02
262.47	0.50	136.45	0.05	152.79	0.09	114213	570.07	24295	1225.48	6791.7	32.97	13674	67.37	245295	1225.48
330.58	0.80	171.73	0.15	192.11	0.22	145652	727.26	313522	1566.61	8576.1	41.89	17292	85.46	313522	1566.61
406.53	1.16	235.93	0.29	235.93	0.39	180899	903.5	390085	1949.43	10568	51.84	21332	105.66	390085	1949.43

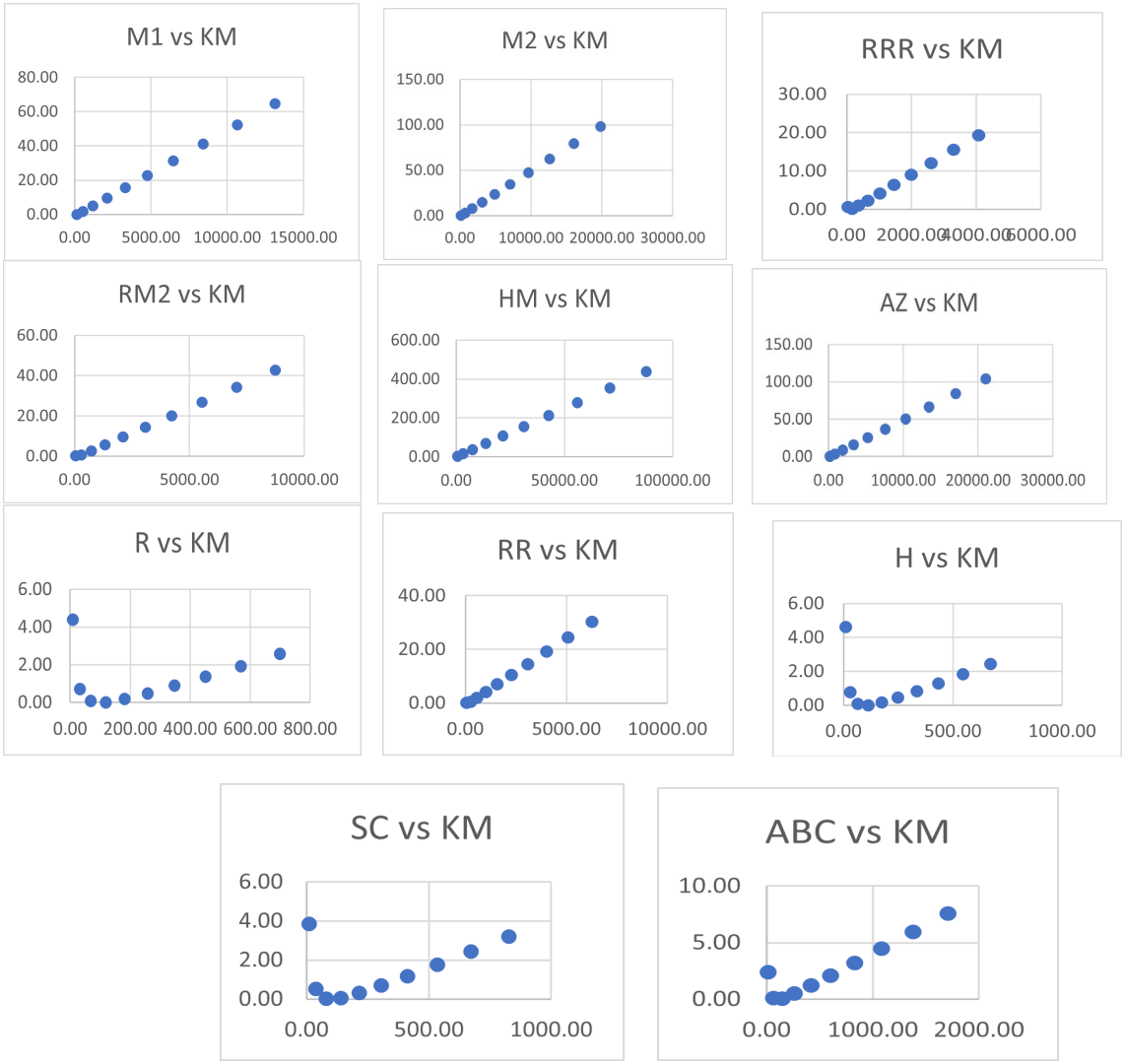

Figure 2. Scatter Plot for Kubelka Munk Function of NiTTFtt (m, n)

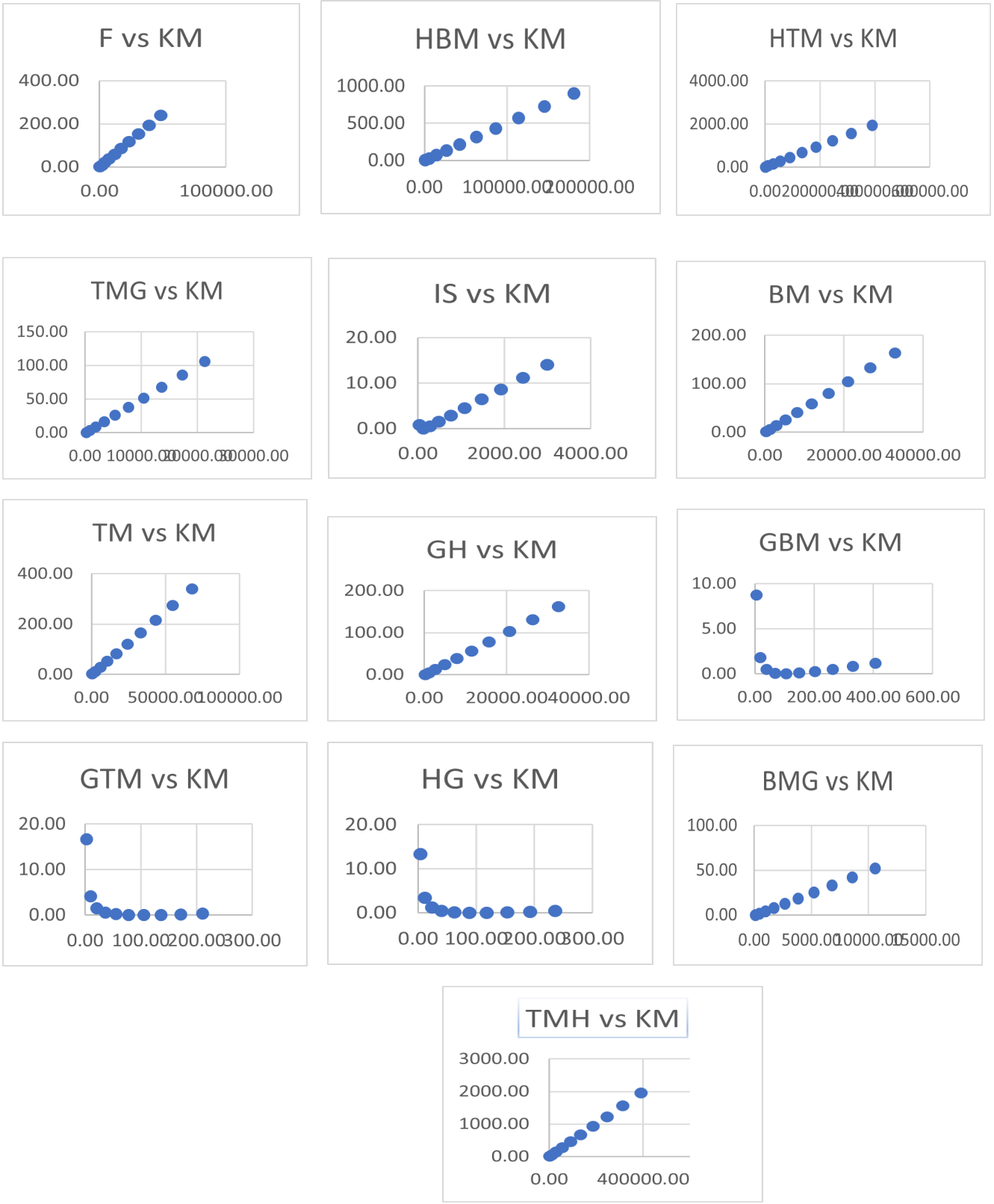

Figure 3. Scatter Plot for Kubelka Munk Function of NiTTFtt (m, n)

Vibrational Frequency (Absorption) and Graph Energy of NiTTFtt Like 2D Sheet

In this subsection, vibrational frequencies are derived for NiTTFtt like 2D sheet based on the total number of vertices and edges of NiTTFtt like 2D sheet with ranges m, n form 1 to 10. These frequencies correspond to the characteristic vibrational modes exhibited by each molecule of NiTTFtt like 2D sheet. The vibrational frequencies obtained, as listed in Table 7, can facilitate the identification of functional groups within the NiTTFtt like 2D sheet molecule [34]. Furthermore, they enable prediction regarding the characteristics of IR spectroscopy associated with NiTTFtt like 2D sheet. Also, statistical prediction between topological indices and vibrational modes of NiTTFtt (m, n) has been done. From statistical analysis, observe that all indices are positively correlated with vibrational frequencies (See Table 8).

Finally, the graph energy of NiTTFtt like 2D sheet with ranges m, n have been obtained for future study of structure property analysis and chemical reactivity (See Table 9).

Table 7. Vibrational modes of NiTTFtt like 2D sheet

m | n	1	2	3	4	5	6	7	8	9	10
1	45	87	129	171	213	255	297	339	381	423
2	96	180	264	348	432	516	600	684	768	852
3	147	273	399	525	651	777	903	1029	1155	1281
4	198	366	534	702	870	1038	1206	1374	1542	1710
5	249	459	669	879	1089	1299	1509	1719	1929	2139
6	300	552	804	1056	1308	1560	1812	2064	2316	2568
7	351	645	939	1233	1527	1821	2115	2409	2703	2997
8	402	738	1074	1410	1746	2082	2418	2754	3090	3426
9	453	831	1209	1587	1965	2343	2721	3099	3477	3855
10	504	924	1344	1764	2184	2604	3024	3444	3864	4284

Table 8. Statistical prediction between δ and Vibrational Modes (VM) OF NiTTFtt like 2D sheet

δ	M_1	M_2	RM_2	HM	AZ	R	RR	RRR
r	0.999998187	0.999981733	0.999935171	0.999971894	0.999992702	0.999991976	0.999998767	0.99999472
δ	H	SC	ABC	F	IS	BM	TM	$G\ H$
r	0.99999146	0.999995201	0.99938161	0.99971451	0.999999227	0.999990341	0.999978469	0.999943649
δ	GBM	GTM	HG	HBM	HTM	BMG	TMG	TMH
r	0.999995156	0.999991971	0.99987551	0.999897866	0.999848212	0.999999958	0.99999746	0.999848212

Table 9. Graph energy of **NiTTFtt** (m, n)

Parameter	Genralized energy value of (m, n)
$(1, n)$	$18.88n - 2.63$
$(2, n)$	$38.54n - 5.77$
$(3, n)$	$58.17n - 10.00$
.	.
.	.
.	.
(m, n)	$19.66mn - 1.09m - 0.78n - 2.05$

Conclusions

In this study, we derive the generalized expressions of NiTTFtt (m,n) of some different valency based topological indices using graph edge partition techniques. We have calculated the structural features of NiTTFtt (m,n) such as KM function, vibrational frequencies and graph energy directly from topological indices values which are significant in IR spectroscopic, band gap energy and topological features of NiTTFtt like 2D sheet. This work reports the strong analysis of spectroscopic applications. To achieve this objectives, we generate valency based topological indices expressions using graph edge partition techniques and show that the strong relationship between the numerical values and vibrational frequencies. Further investigation into spectroscopic analysis can be accelerated using data from this study.

Conflicts of Interest

The authors declares that there is no conflict of interest regarding the publication of this paper.

Acknowledgement

This research was supported by Ministry of Higher Education (MOHE) through the Fundamental Research Grant Scheme (FRGS/1/2022/STG06/UMT/03/4)

References

[1] Plummer, J. (2015). Is metallic glass poised to come of age? *Nature Materials, 14*(6), 553–555.
[2] Xie, J., Boyn, J. N., Filatov, A. S., McNeece, A. J., Mazziotti, D. A., & Anderson, J. S. (2020). Redox, transmetalation, and stacking properties of tetrathiafulvalene-2, 3, 6, 7-tetrathiolate bridged tin, nickel, and palladium compounds. *Chemical Science, 11*(4), 1066–1078.
[3] Heeger, A. J. (2001). Nobel Lecture: Semiconducting and metallic polymers: The fourth generation of polymeric materials. *Reviews of Modern Physics, 73*(3), 681.
[4] Valade, L., de Caro, D., Faulmann, C., & Jacob, K. (2016). TTF [Ni (dmit) 2] 2: From single crystals to thin layers, nanowires, and nanoparticles. *Coordination Chemistry Reviews, 308*, 433–444.
[5] Xie, L. S., Skorupskii, G., & Dinca, M. (2020). Electrically conductive metal–organic frameworks. *Chemical Reviews, 120*(16), 8536–8580.
[6] de Caro, D., Fraxedas, J., Faulmann, C., Malfant, I., Milon, J., Lamère, J. F., Collière, V., & Valade, L. (2004). Metallic thin films of TTF [Ni (dmit) 2] 2 by electrodeposition on (001)-oriented silicon substrates. *Advanced Materials, 16*(9–10), 835–838.
[7] Anderson, J., *et al.* (2022). An intrinsically glassy metallic coordination polymer showing thermally and aerobically robust conductivity.
[8] Kobayashi, A., Fujiwara, E., & Kobayashi, H. (2004). Single-component molecular metals with extended-TTF dithiolate ligands. *Chemical Reviews, 104*(11), 5243–5264.
[9] Kaiser, A. B. (2001). Electronic transport properties of conducting polymers and carbon nanotubes. *Reports on Progress in Physics, 64*(1), 1.
[10] Liu, Y., Rezaei, M., Farahani, M. R., Husin, M. N., & Imran, M. (2017). The omega polynomial and the Cluj-Ilmenau index of an infinite class of the titania nanotubes TiO_2 (m,n). *Journal of Computational and Theoretical Nanoscience, 14*(7), 3429–3432. https://doi.org/10.1166/jctn.2017.6646
[11] Modabish, A., Husin, M. N., Alameri, A. Q., Ahmed, H., Alaeiyan, M., Farahani, M. R., & Cancan, M. (2022). Enumeration of spanning trees in a chain of diphenylene graphs. *Journal of Discrete Mathematical Sciences and Cryptography, 25*(1), 241–25. https://doi.org/10.1080/09720529.2022.2038931
[12] Asif, F., Zahid, Z., Husin, M. N., Cancan, M., Tas, Z., Alaeiyan, M., & Farahani, M. R. (2012). On Sombor indices of line graph of silicate carbide Si_2 C_3-I[p,q]. *Journal of Discrete Mathematical Sciences and Cryptography, 25*(1), 241–251. https://doi.org/10.1080/09720510.2022.2043621
[13] Saidi, N. H. A. M., Husin, M. N., & Ismail, N. B. (2021, July). On the topological indices of the line graphs of polyphenylene dendrimer. In *AIP Conference Proceedings* (Vol. 2365, No. 1). AIP Publishing.
[14] Gao, W., Husin, M. N., Farahani, M. R., Imran, M. (2016). On the edges version of atom-bond connectivity and geometric arithmetic indices of nanocones CNC_K [n]. *Journal of Computational and Theoretical Nanoscience, 13*(10), 6741–6746. https://doi.org/10.1166/JCTN.2016.5622
[15] Husin, M. N., Hasni, R., & Imran, M. (2017). More results on computation of topological indices of certain networks. *International Journal of Networking and Virtual Organisations, 17*(1), 46–63. https://doi.org/10.1504/IJNVO.2017.083543
[16] Vijay, J. S., Roy, S., Beromeo, B. C., Husin, M. N., Augustine, T., Gobithaasan, R. U., & Easuraja, M. (2023). Topological properties and entropy calculation of aluminophosphates. *Mathematics, 11*(11), 2443. https://doi.org/10.3390/math11112443
[17] Saleem, H., Husin, M. N., Ali, S., Hameed, M. S., & Ahmad, Z. (2024). Topology of edge contracted Möbius ladder: Indices and dimension. *Malaysian Journal of Fundamental and Applied Sciences, 20*, 739–758.

https://doi.org/10.11113/mjfas.v20n4.3386
[18] Gowtham, K. J., Husin, M. N. (2023). A study of families of bistar and corona product of graph: Reverse topological indices. *Malaysia Journal of Mathematical Sciences, 17*(4), 575–586. https://doi.org/10.47836/mjms.17.4.04
[19] Gutman, I., & Das, K. C. (2004). The first Zagreb index 30 years after. *MATCH Commun. Math. Comput. Chem, 50*(1), 83–92.
[20] Khalifeh, M. H., Yousefi-Azari, H., & Ashrafi, A. R. (2009). The first and second Zagreb indices of some graph operations. *Discrete Applied Mathematics, 157*(4), 804–811.
[21] Lu, Y., & Zhou, Q. (2022). On hyper-Zagreb index conditions for Hamiltonicity of graphs. *Czechoslovak Mathematical Journal, 72*(3), 653–662.
[22] Ghorbani, M., & Hosseinzadeh, M. A. (2013). The third version of Zagreb index. *Discrete Mathematics, Algorithms and Applications, 5*(04), 1350039.
[23] Buyantogtokh, L., Horoldagva, B., & Das, K. C. (2020). On reduced second Zagreb index. *Journal of Combinatorial Optimization, 39*(3), 776–791.
[24] Hao, J. (2011). Theorems about Zagreb indices and modified Zagreb indices. *MATCH Commun. Math. Comput. Chem, 65*, 659–670.
[25] Gowtham, K. J., Husin, M. N., & Siddiqui, M. K. (2024). Some new bounds on the modified symmetric division deg index. *Malaysian Journal of Mathematical Sciences, 18*(1), 39–50. https://doi.org/10.47836/mjms.18.1.03
[26] Ali, A., Furtula, B., Redžepović, I., & Gutman, I. (2022). Atom-bond sum-connectivity index. *Journal of Mathematical Chemistry, 60*(10), 2081–2093.
[27] Rada, J., Rodríguez, J. M., & Sigarreta, J. M. (2021). General properties on Sombor indices. *Discrete Applied Mathematics, 299*, 87–97.
[28] Furtula, B., & Gutman, I. (2015). A forgotten topological index. *Journal of Mathematical Chemistry, 53*(4), 1184–1190.
[29] Shirdel, G. H., Rezapour, H., & Sayadi, A. M. (2013). The hyper-Zagreb index of graph operations.
[30] Rajasekharaiah, G. V., & Murthy, U. P. (2021). Hyper-Zagreb indices of graphs and its applications. *Journal of Algebra Combinatorics Discrete Structures and Applications, 8*(1), 9–22.
[31] Vukićević, D., & Furtula, B. (2009). Topological index based on the ratios of geometrical and arithmetical means of end-vertex degrees of edges. *Journal of Mathematical Chemistry, 46*, 1369–1376.
[32] Shabbir, A., & Nadeem, M. F. (2022). Computational analysis of topological index-based entropies of carbon nanotube Y-junctions. *J Stat Phys, 188*(31).
[33] Nadeem, M. F., Ishfaq, F., & Shabbir, A. (2024). On resistance distance and Kirchhoff index of cacti networks. *J Stat Phys, 191*(83).
[34] Myrick, M. L., Simcock, M. N., Baranowski, M., Brooke, H., Morgan, S. L., & McCutcheon, J. N. (2011). The Kubelka-Munk diffuse reflectance formula revisited. *Applied Spectroscopy Reviews, 46*(2), 140–165.
[35] Wong, M. W. (1996). Vibrational frequency prediction using density functional theory. *Chemical Physics Letters, 256*(4–5), 391–399.
[36] Gutman, I., Li, X., & Zhang, J. (2009). Graph energy. *Analysis of Complex Networks: From Biology to Linguistics*, 145–174.
[37] Myrick, M. L., Simcock, M. N., Baranowski, M., Brooke, H., Morgan, S. L., & McCutcheon, J. N. (2011). The Kubelka-Munk diffuse reflectance formula revisited. *Applied Spectroscopy Reviews, 46*(2), 140–165.
[38] Gonçalves, I. G., Petter, C. O., & Machado, J. L. (2012). Quantification of hematite and goethite concentrations in kaolin using diffuse reflectance spectroscopy: A new approach to Kubelka-Munk theory. *Clays and Clay Minerals, 60*(5), 473–483.
[39] Landi Jr, S., Segundo, I. R., Freitas, E., Vasilevskiy, M., Carneiro, J., & Tavares, C. J. (2022). Use and misuse of the Kubelka-Munk function to obtain the band gap energy from diffuse reflectance measurements. *Solid State Communications, 341*, 114573.